CD200 Expression on Tumor Cells Suppresses Antitumor Immunity: New Approaches to Cancer Immunotherapy

Anke Kretz-Rommel,* Fenghua Qin,* Naveen Dakappagari,* E. Prenn Ravey,* John McWhirter,* Daniela Oltean,* Shana Frederickson,* Toshiaki Maruyama,* Martha A. Wild,* Mary-Jean Nolan,* Dayang Wu,† Jeremy Springhorn,† and Katherine S. Bowdish[1]*

Although the immune system is capable of mounting a response against many cancers, that response is insufficient for tumor eradication in most patients due to factors in the tumor microenvironment that defeat tumor immunity. We previously identified the immune-suppressive molecule CD200 as up-regulated on primary B cell chronic lymphocytic leukemia (B-CLL) cells and demonstrated negative immune regulation by B-CLL and other tumor cells overexpressing CD200 in vitro. In this study we developed a novel animal model that incorporates human immune cells and human tumor cells to address the effects of CD200 overexpression on tumor cells in vivo and to assess the effect of targeting Abs in the presence of human immune cells. Although human mononuclear cells prevented tumor growth when tumor cells did not express CD200, tumor-expressed CD200 inhibited the ability of lymphocytes to eradicate tumor cells. Anti-CD200 Ab administration to mice bearing CD200-expressing tumors resulted in nearly complete tumor growth inhibition even in the context of established receptor-ligand interactions. Evaluation of an anti-CD200 Ab with abrogated effector function provided evidence that blocking of the receptor-ligand interaction was sufficient for control of CD200-mediated immune modulation and tumor growth inhibition in this model. Our data indicate that CD200 expression by tumor cells suppresses antitumor responses and suggest that anti-CD200 treatment might be therapeutically beneficial for treating CD200-expressing cancers. ***The Journal of Immunology,*** **2007, 178: 5595–5605.**

Tumors have found many ways to evade eradication by the immune system (1). Negative regulation of the immune system by tumor cells has been implicated in the failure of many cancer vaccines (2). Cancer therapy with Abs blocking the negative immune regulator CTLA-4 on T cells has been encouraging (3, 4), suggesting that targeting negative immune regulators in cancer could be therapeutically beneficial. We showed the immune-suppressive molecule CD200 to be up-regulated 1.5- to 5.4-fold on B cell chronic lymphocytic leukemia (B-CLL)[2] cells in all 80 patients examined compared with B cells from healthy donors (5). CD200 is a type 1a transmembrane protein, related to the B7 family of costimulatory receptors, with two extracellular domains, a single transmembrane region, and a cytoplasmic tail with no known signaling motifs (6). It is normally expressed on thymocytes, T and B lymphocytes, neurons, and endothelial cells (7). CD200 binds to its receptor, CD200R, expressed on cells of the monocyte/macrophage lineage and on T lymphocytes (8). Interaction of CD200 with its receptor delivers an inhibitory signal to the macrophage lineage (9, 10), altering cytokine profiles from Th1 to Th2 in MLRs (11) and resulting in the induction of regulatory T cells (12), which are thought to hamper tumor-specific effector T cell immunity (13). Knockout of the CD200 gene in mice and studies with blocking Abs and recombinant Fc fusion proteins containing the CD200 or CD200R extracellular domains have shown that CD200 is a potent immunosuppressant in autoimmune and transplantation settings (9, 14, 15).

Although murine models provide important information with regard to the role of key proteins in immune function, various aspects of the mouse immune system differ dramatically from the human immune system, making inferences from these models unpredictable at times. Particularly in the case of CD200, in contrast to humans where only a single CD200 receptor has been identified, mice have multiple CD200 receptors, including stimulatory and inhibitory receptors (16, 17). Furthermore, none of our anti-human CD200 Abs blocking receptor-ligand interactions cross-reacted with murine CD200. Therefore, to consider the potential therapeutic benefit of targeting human CD200 in a cancer setting, we developed an in vivo NOD/SCID-hu-mouse model evaluating immunosuppression by CD200-expressing human tumor cells on human PBMC (hPBMCs). The model was further used to evaluate the potential therapeutic value of anti-human CD200 Abs.

Materials and Methods

Mice

Four- to six-week-old NOD.CB17-Prkdcscid/J (NOD/SCID) mice were obtained from The Jackson Laboratory. Animals were housed at Perry Scientific. All procedures and protocols were approved by the Perry Scientific Institutional Animal Care and Use Committee.

*Alexion Antibody Technologies, San Diego, CA 92121; and †Alexion Pharmaceuticals, Cheshire, CT 06410

Received for publication July 13, 2006. Accepted for publication January 31, 2007.

The costs of publication of this article were defrayed in part by the payment of page charges. This article must therefore be hereby marked *advertisement* in accordance with 18 U.S.C. Section 1734 solely to indicate this fact.

[1] Address correspondence and reprint requests to Dr. Katherine S. Bowdish, Alexion Antibody Technologies, 3985 Sorrento Valley Boulevard, Suite A, San Diego, CA 92121. E-mail address: kbowdish@alxnsd.com

[2] Abbreviations used in this paper: B-CLL, chronic lymphocytic leukemia; ADCC, antibody dependent cellular cytotoxicity; CDC, complement dependent cytotoxicity; hPBMC, human peripheral blood mononuclear cell.

Library construction, panning, and genetic manipulation of anti-CD200 antibodies

BALB/c mice were immunized alternately with 293-Epstein-Barr nuclear Ag (EBNA) cells transfected with human CD200 and a soluble extracellular portion of human CD200 fused to murine IgG Fc (CD200-Fc). Phage display Ab libraries were made from spleen RNA basically as described by Wild et al. (18), modified for mouse immunoglobulins.

The library of phage displaying Ab Fabs was panned on CD200-Fc either directly coated on microtiter wells (Costar) or captured with anti-mouse IgG Fc Ab (Pierce). The isolated Abs were screened on CD200-Fc and the binding to the cell surface-expressed CD200 was confirmed by flow cytometry analysis. DNA sequences were analyzed and selected Fabs were converted to chimeric IgGs.

Selected Fabs were converted to chimeric Fabs by PCR mutagenesis to fuse mouse variable regions to human constant regions (κ L chain and IgG1 H chain CH1). For expression in mammalian cells, a human CMV immediate early promoter was inserted upstream of the H chain gene. The chimeric Fabs were cloned into an IgG expression vector containing the rest of the human IgG1 H chain constant regions and another human CMV immediate early promoter for expression of the L chain.

Construction of chB7-G2G4

The chimeric Fab B7 was initially cloned in two steps, first into a mammalian expression vector derived from the Lonza vector system bearing IgG1 H chain sequences and, subsequently, the IgG1 H chain sequences were replaced with IgG2G4 coding sequences (19). To switch the IgG1 coding sequences in B7 to IgG2G4 coding sequences, the IgG1 region from the *Pin*AI site in the human CH1 region through the stop codon to a *Bam*HI site located after the SV40 pA was replaced with the corresponding region of an IgG2G4 coding sequence, which also bears a *Pin*AI site at the same position in the CH1 region and was followed by a similar SV40pA sequence. B7 and an IgG2G4-bearing clone were therefore digested with *Age*I and *Bam*HI (*Age*I is an isoschizomer of *Pin*AI), and a 1752-bp fragment from the IgG2G4-bearing clone was used to replace the corresponding region of C2AB7-6 and generate clone 21.

The remainder of the IgG1 CH1 region from the end of the variable region to the *Age*I site was converted to an IgG2G4 format by using overlap PCR. Primers were used in a PCR with an IgG2G4-expressing clone as the template to generate a fragment containing the desired CH1 region. Other primers were used with the chimeric Fab C2aB7 as the template to generate the murine H chain variable region. These fragments were used in overlap PCR, the resulting fragment was digested with *Xho*I and *Age*I, and a 458-bp fragment was used to replace the corresponding *Xho*I/*Age*I fragment in clone 21 to generate chB7-G2G4.

Humanization of anti-CD200 mAb chB7-G1

Compartmentalized framework sequences, defined as FR1, FR2, FR3, and FR4, were replaced individually by the corresponding framework sequences from different human H chain and L chain Ig variable regions. The murine CDRs of chB7-G1 in both the H and L chains of the humanized C2aB7 were maintained. Humanized B7 H chain variable region sequences and L chain region sequences were generated by overlap PCR with mutagenic oligonucleotides primers encompassing the regions to be altered, using chB7-G1 as the template. Primers were engineered to introduce human framework sequences as well as a *Hin*dIII site, a Kozak sequence (GCCGCCACCATGG) to enhance translation initiation, and a secretion signal sequence, and to fuse the humanized B7 variable H chain region in frame with the first six amino acids (spanning an *Apa*I restriction site) of the human γ 1 (G1) CH1 region in the case of the H chain or to fuse the humanized B7 variable L chain in frame with the first amino acid (covering a *Bsi*WI restriction site) in the human constant κ-chain (Cκ). The PCR fragments were TA cloned into pCR2.1 vector using a TOPO TA cloning kit (Invitrogen Life Technologies). DNA was isolated and sequenced for confirmation. For H chain cloning, the resulting plasmid was digested with *Hin*dIII and *Apa*I, and the restriction fragment encoding the humanized B7 variable region H chain was cloned into the plasmid pEE6 (Lonza) encoding a human G1 constant region. For L chain cloning, the pCR2.1 vector encoding the hB7V1 variable L chain was digested with *Hin*dIII/*Bsi*WI and the restriction fragments were cloned into the pEE12 vector (Lonza) encoding a human constant κ-chain. To generate a double gene vector encoding both the humanized L chain and H chain, the vectors encoding the humanized L chain or humanized H chain were digested with *Not*I/*Bam*HI and the resulting fragments encoding the respective Ab chains were ligated.

Antibody production

For in vitro studies, anti-CD200 Abs were produced by transient transfections of 293 cells with the appropriate Ab construct. For in vivo studies, anti-CD200 Abs and the negative control mAb ALXN4100, recognizing anthrax toxin, were produced in serum-free medium by stable Chinese hamster ovary clones containing the appropriate Ab construct. Ab in supernatant was purified by HPLC on protein A columns. Ab concentrations were determined by OD. Endotoxin levels were below the level of detection as demonstrated by the *Limulus* amebocyte lysate test (Cambrex).

Fluorescent bead assay

Carboxylate-modified TransFluorSpheres (488/645 nm, 1.0 μm; Molecular Probes) were coated with CD200Fc (5). For adhesion to ligand-coated fluorescent beads, CD200R-transfected 293-EBNA cells (5×10^6/ml) were resuspended in Tris-sodium-BSA buffer (20 mM Tris-HCl (pH 8.0), 150 mM NaCl, 1 mM $CaCl_2$, 2 mM $MgCl_2$, and 0.5% BSA). Fifty thousand cells were preincubated with or without anti-CD200 Abs for 10 min at room temperature in a 96-well V-bottom plate. The ligand-coated fluorescent beads (20 beads/cell) were added and the suspension was incubated for 30 min at 37°C. After washing, the cells were resuspended in Tris-sodium-BSA buffer. The percentage of cells bound to ligand-coated beads was measured by a FACSCalibur flow cytometer in FL-3.

Mixed lymphocyte reactions

Mixed lymphocyte reactions were set up in 24-well plates using 500,000 monocyte-derived dendritic cells and 1×10^6 responder cells (T cells) as described in McWhirter et al. (5). Responder cells were T cell-enriched lymphocytes purified from peripheral blood by Histopaque separation. Five hundred thousand hPBMCs from patients with B-CLL were added to the dendritic cells in the presence or absence of 10 μg/ml anti-CD200 Ab 2–4 h before lymphocyte addition. Patient samples added to the culture contained $>$80% $CD19^+CD5^+CD38^+CD200^+$ B-CLL cells. Supernatants were collected after 48 and 68 h and analyzed for the presence of cytokines by ELISA (5). Matched capture and detection Ab pairs for each cytokine were obtained from R&D Systems, and a standard curve for each cytokine was produced using recombinant a human cytokine.

Off-rate assay

For off-rate studies, the respective Abs were labeled using a Zenon kit (Molecular Probes). Primary human B-CLL cells obtained from The Scripps Cancer Center (La Jolla, CA) were blocked with a FcR blocking reagent and a saturating amount of Ab was added to the cells. After 30 min of incubation on ice, cells were washed and placed at room temperature and the presence of an anti-CD200 Ab on the cell surface was determined at various time points using a FACSCalibur flow cytometer.

Creation of stable CD200-expressing cancer cell lines

Stable CD200-expressing RAJI and Namalwa cell lines were generated using the ViraPower lentiviral expression system (Invitrogen Life Technologies). CD200 cDNA was isolated from primary human B-CLL cells obtained from A. Savan (The Scripps Cancer Center) by RT-PCR. The PCR product was cloned into the Gateway entry vector pCR8/GW/TOPO-TA (Invitrogen Life Technologies). Clones with the correct sequence (compared with National Center for Biotechnology Information sequence identifier NM_005944) were recombined in both the sense and antisense orientations into the lentiviral vector pLenti6/UbC/V5/DEST (Invitrogen Life Technologies) containing the human ubiquitin C promoter using Gateway technology. High-titer vesicular stomatitis virus G protein-pseudotyped lentiviral stocks were produced and cultured with RAJI (American Type Culture Collection (ATCC)) or Namalwa (ATCC) cells. Two days later, the infected cells were analyzed for CD200 cell surface expression by flow cytometry. In all transductions, $\geq$70% of the cells were $CD200^+$, whereas CD200 was undetectable in the parental cell lines and in cells transduced with the viruses containing the reversed orientation CD200 construct. Stable clones were produced by limiting dilution. Absolute numbers of CD200 molecules per cell on the transfected cell lines were assessed by flow cytometry using QIFIKIT according to the manufacturer's instructions and compared with the expression levels on primary B-CLL cells.

Isolation of hPBMCs from human peripheral blood

Peripheral blood was drawn from healthy human donors at the San Diego Blood Bank after informed consent and Institutional Review Board approval. Peripheral blood from B-CLL patients was obtained from Dr. A. Saven (The Scripps Clinic, La Jolla, CA) after informed consent and

Institutional Review Board approval. hPBMCs were isolated using a Histopaque gradient. RBCs were lysed using NH_4Cl.

Depletion of T cells or monocytes/macrophages

Monocytes, macrophages, and dendritic cells were simultaneously depleted from hPBMCs by cell sorting with magnetic beads coated with CD14 Abs (Miltenyi Biotec) and CD11c as per the manufacturer's instructions. T cells were depleted with magnetic beads coated with CD3. After sorting the cells, the depleted hPBMCs were resuspended in the same volume of medium as the equivalent number of undepleted hPBMCs before injection into animals. Successful depletion (>90%) was verified by FACS analysis.

Transfer of cells into NOD/SCID mice

Mice were uniquely numbered with ear tags and were randomized into the required number of treatment groups based on their body weight on the day before cell injection. Four million tumor cells and 2×10^6 to 10×10^6 fresh hPBMCs in a total volume of 200 μl of RPMI complete medium were injected s.c. in a shaved area on the back of the mice.

Antibody dose, schedule, and administration

In some studies one-tenth of the dose of Ab indicated was mixed with 4×10^6 tumor cells and 5–10×10^6 hPBMCs in a total volume of 200 μl and administered s.c. Animals subsequently received six doses of Ab as indicated, administered i.v. two times a week for 3 wk. In another set of studies, Ab was only administered i.v. starting 7 days after cell injection.

Tumor volume measurements

Tumor length and width were measured using a caliper three times per week by personnel blinded to the group design. Tumor volumes were calculated as follows: (length $\times$ width $\times$ width)/2. If a second tumor occurred in a given mouse, both tumor volumes were measured and their volumes added together. Tumor growth inhibition was calculated by 100 $-$ ((mean tumor volume anti-CD200 Ab treated groups/mean tumor volume control mAb-treated groups) $\times$ 100).

FACS analysis

At the end of some in vivo experiments, tumor cells from randomly selected mice were isolated and resuspended in FACS buffer (PBS, 1% BSA, and 0.05% NaN_3) at 5×10^6 cells/ml. The anti-CD200 Ab C1a10 was labeled with an Alexa Fluor 488-conjugated Zenon label (Invitrogen Life Technologies) according to the manufacturer's instructions. The Ab recognizes a different epitope than the anti-CD200 Ab chB7-G1. Cell staining of CD200 molecules was detected using a FACSCalibur flow cytometer (BD Biosciences).

Serum cytokine analysis

In one in vivo study mouse serum was collected by retroorbital puncture before the start of the study and on day 8 after cell injection. The presence of human cytokines was determined by flow cytometry using a cytokine bead array (BD Biosciences) and a 1/2 serum dilution according to the manufacturer's instruction.

Statistical analysis

Differences in tumor growth between the anti-CD200-treated and control groups were determined using the Wilcoxon rank sum test, with $p < 0.05$ considered significant. Statistical analysis was performed by the statistician S. Talwalker (T'Walker Consulting).

Immunohistochemistry

Four randomly selected tumors from each group at the end of some of the animal studies were removed, embedded in OCT, and snap frozen. The samples were sectioned at 5 μm in a Leica Cryostat. The sections were fixed in cold acetone and cold formalin before immunohistochemistry staining.

The slides were stained on the Ventana Medical Systems Benchmark XT IHC machine using a streptavidin detection system. A streptavidin-conjugated CD8 Ab (Cell Marque), CD4 Ab (Novacastra), or CD11c Ab (Serotec) was applied, followed by biotinylated IgG, HRP-conjugated streptavidin, and diaminobenzidine. Slides were counterstained with hematoxylin.

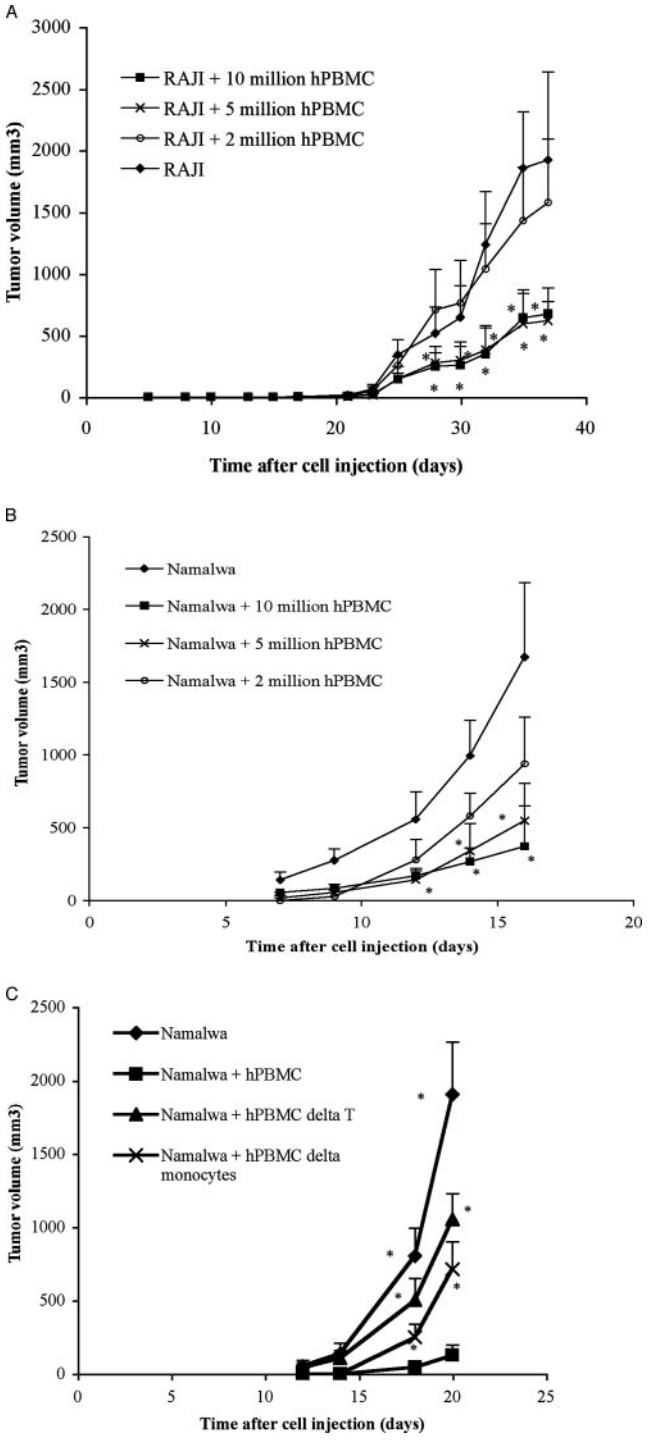

FIGURE 1. hPBMCs inhibit tumor growth of RAJI and Namalwa cells. *A*, Tumor growth of RAJI cells in the absence or presence of 2, 5, or 10×10^6 hPBMC. All mice that were injected with RAJI cells (eight of eight) or RAJI cells with 2×10^6 hPBMC (nine of nine), 5×10^6 hPBMC (nine of nine), or 10×10^6 hPBMC (eight of eight) developed tumors by the end of the study. *B*, Tumor growth of Namalwa cells in the absence or presence of 2, 5, or 10×10^6 hPBMC. All mice that were injected with Namalwa cells (eight of eight) or Namalwa cells with 5×10^6 hPBMC (nine of nine) or 10×10^6 hPBMC (eight of eight) developed tumors. Eight of nine mice injected with Namalwa cells with 2×10^6 hPBMC grew tumors by the end of the study. *C*, Tumor growth of Namalwa cells in the absence or presence of 10 million each of hPBMCs, T cell-depleted hPBMCs, or monocyte/macrophage-depleted hPBMCs. In all experiments, hPBMC and 4×10^6 tumor cells were mixed and injected s.c. into NOD/SCID mice. hPBMCs from a single donor were used within a given experiment. Error bars represent mean $\pm$ SEM; $*$, $p < 0.05$.

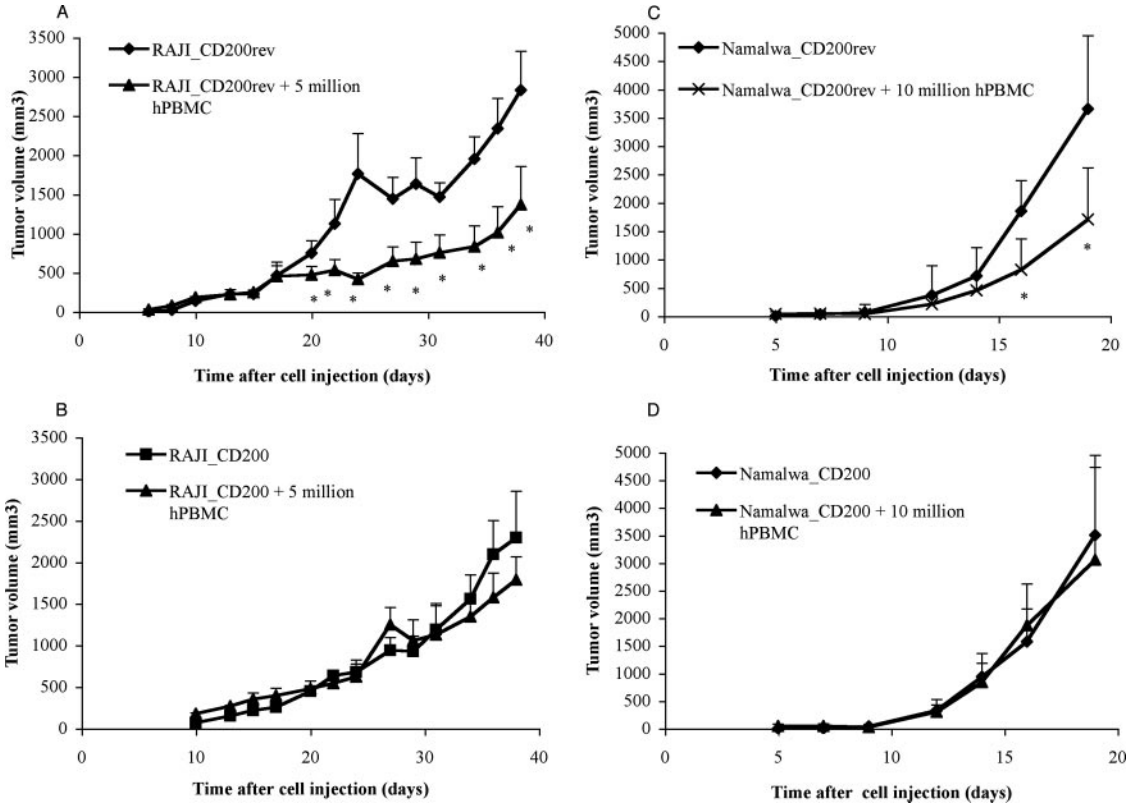

FIGURE 2. Effect of CD200 on tumor rejection by hPBMCs. *A*, Tumor growth of RAJI_CD200rev cells in the presence or absence of hPBMCs. All mice that were injected with RAJI_CD200rev cells (eight of eight) or RAJI_CD200rev cells with hPBMCs (nine of nine) developed tumors by the end of the study. *B*, Tumor growth of RAJI_CD200 cells in the presence or absence of hPBMCs. All mice in RAJI_CD200 (nine of nine) or RAJI_CD200 with hPBMCs (nine of nine) developed tumors by the end of the study. *C*, Tumor growth of Namalwa_CD200rev cells in the presence (tumor incidence: eight of eight) or absence (tumor incidence: eight of eight) of hPBMCs. *D*, Tumor growth of Namalwa_CD200 cells in the presence (tumor incidence: eight of eight) or absence (tumor incidence: nine of nine) of hPBMCs. In all experiments, 5–10 $\times$ 10^6 hPBMCs and 4 $\times$ 10^6 tumor cells were mixed and injected s.c. into NOD/SCID mice. hPBMCs from a single donor were used within a given experiment. Error bars represent mean $\pm$ SEM; $n = 10$ per group. $*$, $p < 0.05$.

Results

Expression of human CD200 on tumor cell lines prevents the rejection of tumor cells by hPBMCs in a NOD/SCID hu-mouse model

To evaluate in vivo whether CD200 expression on human tumor cells such as B-CLL cells suppresses the human immune system, we established a model demonstrating that hPBMCs can reject tumor cells lacking CD200 expression. Despite attempts by many researchers, primary B-CLL cells rarely form tumors when injected into immunodeficient mice. Furthermore, because B-CLL cell lines forming xenografts were not available and none of the hematological cancer-derived cell lines maintain CD200 expression in culture, the human Burkitt's lymphoma cell lines RAJI (20) and Namalwa (21) were chosen as substitutes. Freshly isolated hPBMCs, regardless of HLA-type, were injected simultaneously with RAJI or Namalwa cells s.c. into immune-deficient NOD/SCID mice, and tumor growth was compared. An allogeneic model system supports the vigorous lymphocyte-mediated killing of cancer cells within the limited lifespan of hPBMCs in this model and provides a rigorous evaluation of potential immune suppression mediated by CD200. As shown in Fig. 1*A*, tumor growth of RAJI cells was significantly reduced in a dose-dependent manner by hPBMCs ($p < 0.003$). Tumor growth was inhibited up to 76% in the groups that received 5 or 10 million hPBMCs. In the Namalwa model (Fig. 1*B*), the presence of 5 or 10 million hPBMCs significantly inhibited tumor growth (up to 75%) over a sustained period of time. Due to the limited lifespan of human immune cells in the model, nearly all mice eventually succumb and form tumors. The injection of 2 million hPBMCs did not significantly affect tumor growth in either model. Both models were repeated multiple times with eight different donors, resulting in a 50–98% tumor growth reduction depending on the donor lymphocytes (data not shown). Rejection of the tumor by hPBMCs required both T cells and monocyte or myeloid dendritic cells, because the elimination of either cell population resulted in a significantly lower tumor growth reduction compared with the unmanipulated hPBMCs (Fig. 1*C*).

To explore the effect of CD200 expression on tumor cells, RAJI and Namalwa cells were transduced with a cDNA encoding human CD200 (clones designated RAJI_CD200 or Namalwa_CD200) or with a reverse orientation CD200 cDNA as a negative control (clones designated RAJI_CD200rev or Namalwa_CD200rev), and stable CD200-expressing clones were selected. CD200 expression on the selected clones was similar to the expression level observed on human B-CLL cells as determined by flow cytometry. B-CLL cells expressed 50,000–200,000 copies/cell, while RAJI_CD200 and Namalwa_CD200 cells expressed ~170,000 copies per cell. Furthermore, we evaluated whether CD200R is expressed in normal hPBMCs at similar levels as in B-CLL patients. Both healthy donors and B-CLL patients showed considerable CD200R expression with an average of 30% of all PBMCs expressing CD200R, including T cells and myeloid cells. Although B-CLL patients have

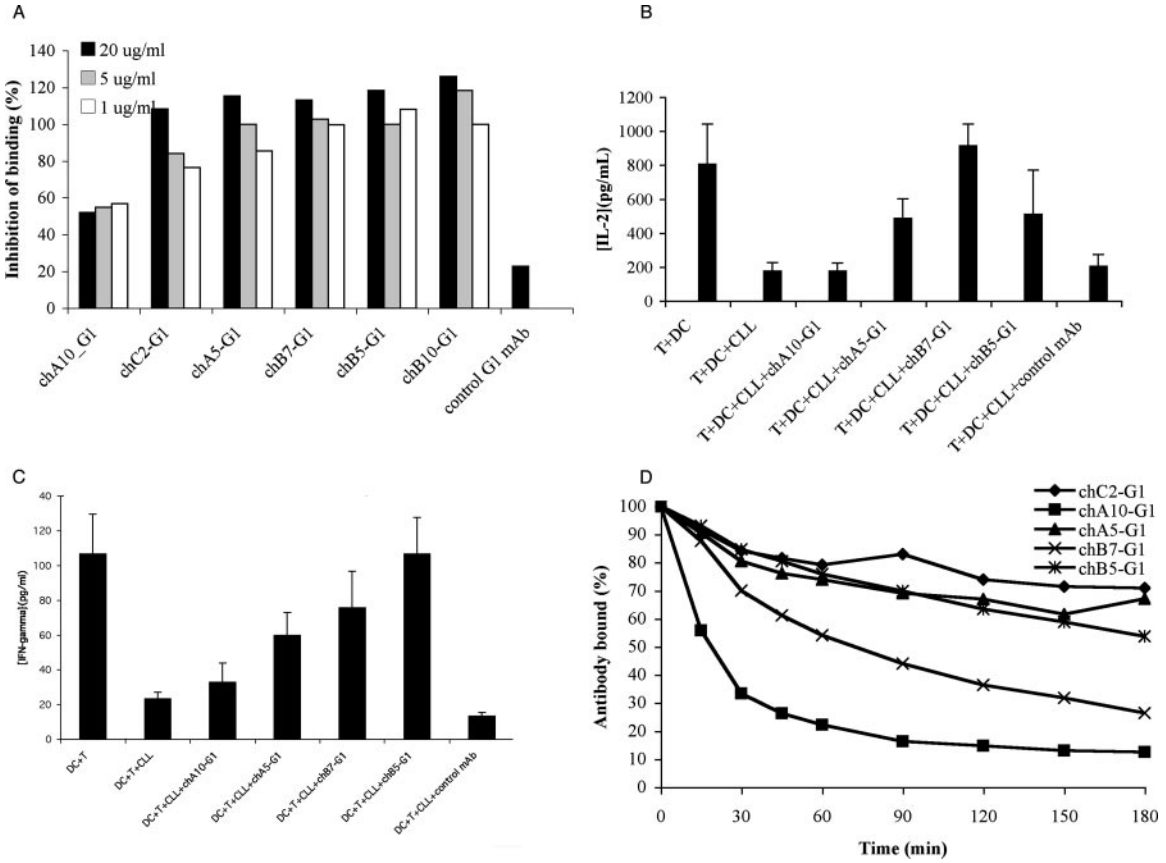

FIGURE 3. *A*, Selection of antagonistic anti-CD200 Abs by bead assay. The blocking by anti-CD200 Abs of the interaction of CD200R on cells with CD200 coated on fluorescent beads was determined by FACS. *B*, MLR. IL-2 in supernatants of cultures with dendritic cells, allogeneic T cells, and primary B-CLL cells (hPBMC from a single patient) in the presence or absence of 10 μg/ml Ab was determined by ELISA, Error bars represent mean $\pm$ SD of triplicates. One typical experiment of five using different B-CLL patient samples is shown. *C*, MLR. IFN-γ in the supernatants of cultures with dendritic cells, allogeneic T cells, and primary B-CLL cells from a single patient in the presence or absence of 10 μg/ml Ab was determined by ELISA. Error bars represent mean $\pm$ SD; $n = 3$. *D*, The off-rate of allophycocyanin-labeled anti-CD200 Abs on primary hPBMCs from a B-CLL patient was determined by FACS over a 3-h time period.

considerably reduced numbers of T cells, the number of myeloid cells was similar in our analysis, which constitutes the bulk of CD200R-expressing cells. Our model therefore appears to adequately represent CD200 and CD200R expression.

Tumor growth of the RAJI or Namalwa cells was not altered by the presence of CD200 or the vector containing the reverse orientation CD200 cDNA (data not shown). As observed with the nontransduced tumor cells (Fig. 1*A*), the tumor growth of RAJI_CD200rev was reduced by hPBMCs (Fig. 2*A*). In contrast, hPBMCs from the same donor could not significantly reduce tumor growth in the groups that received CD200-expressing RAJI cells (CD200_RAJI model) (Fig. 2*B*). Similarly, CD200 expression on Namalwa cells (CD200_Namalwa model) prevented the inhibition of tumor growth by hPBMCs (Fig. 2*D*) seen with Namalwa_CD200rev cells (Fig. 2*C*).

These results demonstrate that the presence of CD200 on tumor cells such as RAJI and Namalwa prevents hPBMCs from inhibiting tumor growth. The data indicate that the CD200_RAJI and CD200_Namalwa models provide robust systems for testing the antitumor efficacy of antagonistic anti-CD200 Abs and a preclinical model for evaluating the potential therapeutic value in targeting CD200.

Selection of antagonistic anti-CD200 antibodies

We previously isolated a panel of murine anti-human CD200 Fabs by panning a phage display library derived from mice immunized with CD200-transfected cells and recombinant human CD200Fc on recombinant human CD200Fc (5). Selected Fabs were converted to chimeric mouse/human IgG1s and evaluated for their ability to block the interaction of CD200 with CD200R. Fig. 3*A* shows in a flow cytometric bead assay that the anti-CD200 Abs chA5-G1, chB7-G1, chB5-G1, and chB10-G1 completely blocked the interaction of CD200 with CD200R when used at 5 μg/ml, while the negative control Ab showed little effect on the ligand/receptor interaction. chA10-G1 showed only weak inhibition of the receptor/ligand interaction.

We previously demonstrated that the presence of CD200-expressing B-CLL cells in human MLR reduces Th1 cytokine production (5). The ability of the panel of chimeric anti-CD200 Abs to inhibit this cytokine shift was assessed (Figs. 3, *B* and *C*). In MLR, chB7-G1 completely prevented down-regulation of the Th1 cytokine IL-2 by B-CLL cells and chB5-G1 and chA5-G1 significantly inhibited such down-regulation, whereas chA10-G1 and the negative control mAb did not affect the cytokine profile. Similarly, IFN-γ production was down-regulated in the presence of B-CLL cells and substantially inhibited by chB7-G1, chB5-G1, and chA5-G1 (Fig. 3*C*).

The ability of the Abs to mediate Ab-dependent cellular cytotoxicity (ADCC) was tested on 293 cells transfected to express human CD200 protein. All Abs showed moderate but significant ADCC activity compared with the negative control Ab ($p < 0.05$ as calculated by Student's t test; data not shown). Differences in

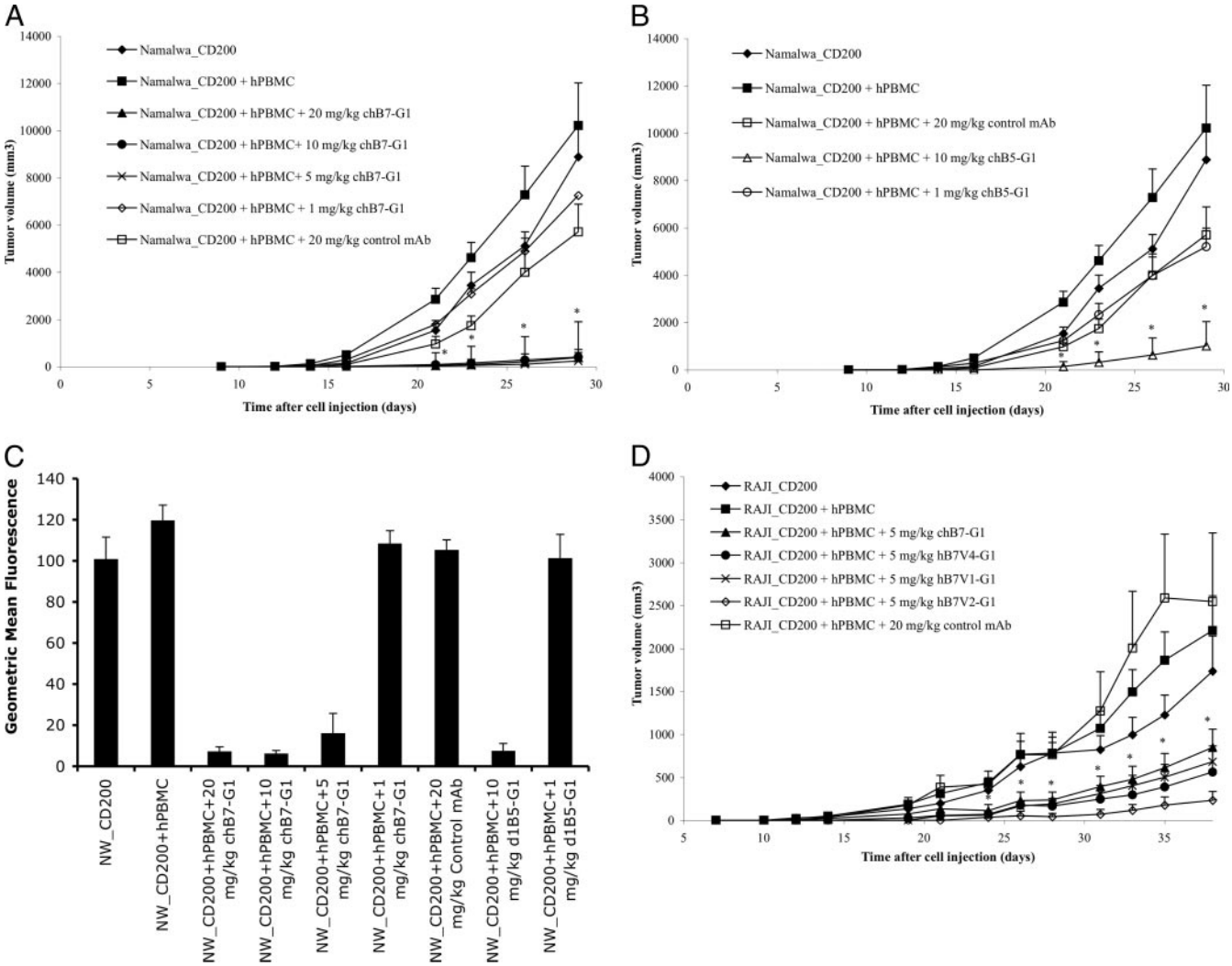

FIGURE 4. Antagonistic anti-CD200 Abs inhibit tumor growth in the CD200_Namalwa and CD200_RAJI hPBMC models. *A*, Tumor growth in the CD200_Namalwa model with or without chB7-G1 treatment; All mice grew tumors in the Namalwa_CD200 group (nine of nine), the Namalwa_CD200 with hPBMC group (10 of 10), the 20 mg/kg control Ab group (10 of 10), and the 1 mg/kg chB5-G1 group (10 of 10). Six of ten mice grew tumors in the 20, 10, and 5 mg/kg chB7-G1 groups respectively, and eight of 10 mice in the 1 mg/kg chB7-G1 group developed tumors. Error bars represent mean ± SEM, ∗, $p < 0.00001$. *B*, Tumor growth in the CD200_Namalwa model with or without chB5-G1 treatment. All mice grew tumors in the 1 mg/kg chB5-G1 group (10 of 10), as did eight of 10 mice in the 10 mg/kg chB5-G1 group. Error bars represent mean ± SEM, ∗, $p < 0.00001$. *C*, CD200 expression on day 27 in the CD200_Namalwa (NW_CD200) model. At the end of the study, tumors from three mice per group were removed and single cells were isolated and analyzed for the presence of CD200 by staining with an Alexa Fluor 488-labeled anti-CD200 Ab. Values represent mean ± SD. *D*, Tumor growth in the CD200_RAJI model. Tumor incidence is 10 of 10 mice for the RAJI_CD200 and RAJI_CD200 plus hPBMC groups, eight of 10 in the 5 mg/kg chB7-G1 group, five of 10 in the 5 mg/kg hB7V4-G1 and 5 mg/kg hB7V2-G1 groups, nine of 10 in the 5 mg/kg hB7V1-G1 group, and seven of eight in the 20 mg/kg control Ab group. Error bars represent mean ± SEM; ∗, $p < 0.001$. In all experiments the hPBMCs and tumor cells were mixed with one-tenth of the indicated Ab dose and injected s.c. into NOD/SCID mice. Subsequently, mice were injected i.v. with the indicated doses twice a week for 3wk.

ADCC and complement dependent cytotoxicity (CDC) activity in vivo have been largely attributed to differences in Ab off-rate for Abs with the same constant region and Ag specificity (22). Although chC2-G1, chA5-G1, and chB5-G1 had the slowest off-rates, chA10-G1 exhibited the fastest off-rate and the chB7-G1 off-rate fell between that chA10-G1 and the other candidates (Fig. 3*D*). Based on their ability to block the cytokine shift in MLR and their off-rate differences, we chose chB7-G1 and chB5-G1 as our candidates to test in the CD200_RAJI and CD200_Namalwa hPBMC models.

Anti-CD200 Ab treatment inhibits tumor growth in the CD200_Namalwa and CD200_RAJI models

The ability of the anti-CD200 Abs chB5-G1 and chB7-G1 to inhibit tumor growth was tested in the CD200_Namalwa model. Neither Ab cross-reacts with murine CD200; therefore, no murine syngeneic models can be used. chB7-G1 was given at four doses ranging from 1 to 20 mg/kg. Due to the limited availability of hPBMCs from a single donor, chB5-G1 Ab was only tested at two doses, 1 and 10 mg/kg. In the first studies, one-tenth of the indicated Ab dose was given at the time of tumor cell and hPBMC injection, after which the mice were treated i.v. twice per week for 3 wk at the indicated dose.

Treatment with doses of 5, 10, or 20 mg/kg chB7-G1 or 10 mg/kg chB5-G1 significantly ($p < 0.0001$) inhibited tumor growth compared with the negative control Ab from day 23 to the end of the study (day 28) (Fig. 4, *A* and *B*), where 20 mg/kg dosing of negative control mAb did not affect tumor growth relative to the group that received no hPBMCs. Tumor growth in the group that received Namalwa_CD200 cells and hPBMCs was somewhat

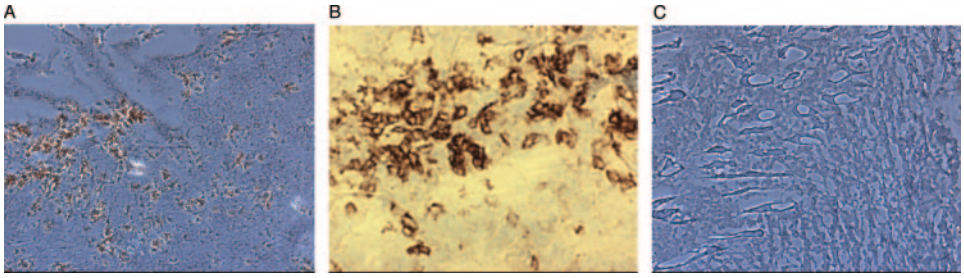

FIGURE 5. $CD8^+$ T cells are found in tumors from mice treated with anti-CD200 Ab but not in mice that received the control Ab. Tumors from mice described in Fig. 4 were snap frozen and slides were prepared and stained with anti-human CD8 Ab. *A* and *B*, Representative tumor from mouse treated with 20 mg/kg chB7-G1 at ×10 or ×40 magnification, respectively. *C*, Representative tumor from control mouse that received 20 mg/kg control Ab (×10 magnification). Stained cells on a 1-cm^2 field on each section were counted. Slides from four different tumors per group were examined. More than 25 $CD8^+$ T cells per field were observed in the positive samples.

higher than that in the control Ab group in this study. Once mean tumor volumes are very large, more variation is observed. In multiple studies with similar design, there is either no increased tumor growth in the presence of hPBMCs or the differences did not reach statistical significance. Tumor growth inhibition was not significantly different among the 5–20 mg/kg dose groups for chB7-G1. The inhibition (compared with the control mAb group) at day 28 was 95, 93, or 93% in the groups dosed with 5, 10, or 20 mg/kg chB7-G1, respectively. Dosage with 10 mg/kg chB5-G1 resulted in 82% tumor growth inhibition. The 1 mg/kg chB7-G1 or chB5-G1 dose did not significantly inhibit tumor growth. These data suggest that either the anti-CD200 Abs mediate ADCC or CDC of the tumor cells or that anti-CD200 treatment can block the immune suppression of CD200-expressing tumor cells. A direct cytotoxic effect of the anti-CD200 Ab in the absence of immune cells was excluded in vitro. The anti-CD200 Abs did not directly block proliferation or induce apoptosis in RAJI_CD200 or Namalwa_CD200 cells, as expected in the absence of any known signaling domain or docking motif in the cytoplasmic tail of CD200 (data not shown).

Flow cytometric analysis of tumor cells at the study's end revealed a large reduction in CD200 cell surface expression in tumors from mice dosed with 5–20 mg/kg anti-CD200 Ab compared with tumors in mice from the control groups (Fig. 4*C*). The detecting Ab recognized a different or slightly overlapping epitope than the CD200 Ab used for treatment. Although not strictly quantitative, the result indicates that the loss of CD200 detection was not a result of an inability of the detecting Ab to bind CD200 due to a prebound anti-CD200 Ab but was indeed a result of the loss of CD200 on the cell surface. In contrast, no reduction was seen in mice that received 1 mg/kg doses of chB5-G1 or chB7-G1, indicating that CD200 expression of the cells is stable in the in vivo environment but can be down-regulated upon treatment.

The dosing experiment described above was repeated in the CD200_RAJI model with similar results (data not shown). For human therapeutic use, it is desirable to humanize the Ab by replacing murine amino acids in the chimeric Ab framework with the corresponding human framework amino acids where possible. Three humanized Abs derived from chB7-G1 were produced and evaluated for their efficacy in inhibiting tumor growth compared with the parental chimeric Ab in the CD200_RAJI (Fig. 4*D*) and CD200_Namalwa (data not shown) models. Affinities of the humanized Abs were comparable to the parental Ab. Treatment with negative control Ab did not inhibit tumor growth, whereas groups treated with any of the three humanized anti-CD200 Abs at 5 mg/kg had significantly reduced ($p < 0.001$) tumor burden from day 24 until the end of the study. All humanized Abs showed >75% tumor growth inhibition, while treatment with the parental chimeric chB7-G1 Ab resulted in 70% tumor growth inhibition. This demonstrates that the humanized versions of chB7-G1 are effective in inhibiting tumor growth in the CD200_RAJI model. Humanized Ab hB7V2-G1 was most effective, with only 5% tumor growth compared with the control Ab-treated group. The anti-CD200 Abs did not enhance hPBMC-mediated tumor growth inhibition of RAJI or Namalwa cells that do not express CD200, indicating that the Ab effect is specific to CD200-expressing tumor cells (data not shown).

Immunohistochemistry staining of a limited number of tumors showed that in tumors from mice that received anti-CD200 Ab, a large number of $CD8^+$ T cells (>25 T cells/field) was present in the small tumors found at the end of the study (Fig. 5, *A* and *B*), while no $CD4^+$ or $CD11c^+$ cells could be detected. In contrast, no human immune cells were found at the end of the study in tumors from mice that received hPBMCs and the control Ab (Fig. 5*C*), confirming activation or retention in the tumor environment of the human immune cells in the anti-CD200 treated mice and providing mechanistic support for CTL activity against the tumor. Furthermore, in one study using the CD200_Namalwa model, the presence of human cytokines (IL-2, IFN-γ, IL-4, IL-10, TNF-α, IL-8, IL-6, IL-12) in mouse serum 8 days after cell injection was evaluated by flow cytometry in a randomly selected number of mice treated with humanized anti-CD200, control mAb, or vehicle control as a readout for immune activation. Only IFN-γ was detectable with the anti-CD200-treated group showing elevated levels of IFN-γ (146 ± 26 pg/ml) compared with the control mAb-treated group (94 ± 7 pg/ml) or vehicle control (110 ± 22). Although the differences did not reach statistical significance, the trend suggests cytotoxic T cell activation and the killing of tumor cells. In addition, we evaluated the presence of antitumor Abs in the serum of mice by flow cytometry. No antitumor Abs were detectable, suggesting that there was no strong humoral antitumor response.

Tumor growth inhibition as a result of anti-CD200 Ab treatment is immune mediated

When CD200 is expressed on tumor cells, tumor growth inhibition by anti-CD200 Abs with a G1 constant region could simply be mediated through ADCC or CDC and not through the postulated blocking of CD200-mediated immune suppression. To evaluate whether an Ab without an effector function can inhibit tumor growth in the CD200_Namalwa model, an Ab with an effectorless constant region was made. chB7-G2G4 carries a hybrid constant region composed of a fusion of G2 and G4 in the hinge of the C-regions (19). As observed with other Abs carrying a G2G4 constant region (19), chB7-G2G4 did not bind to FcγR1, or FcγR2, nor did it mediate complement activation or ADCC (data not shown). Mice were treated with either chB7-G2G4 or chB7-G1 at

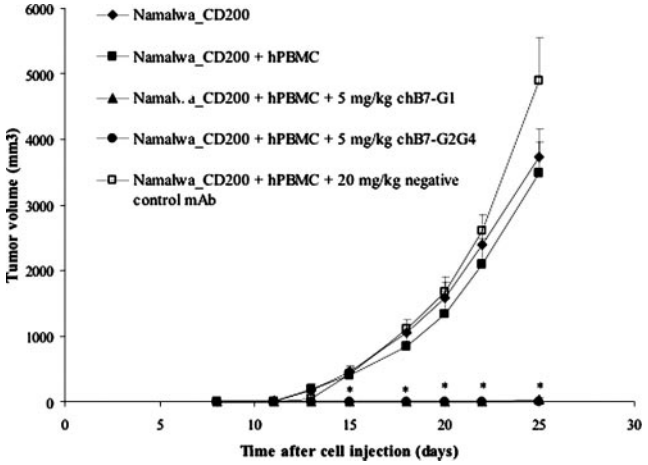

FIGURE 6. Anti-CD200 Ab without effector function (chB7-G2G4) inhibits tumor growth in the CD200_Namalwa hPBMC model. Tumor growth in NOD/SCID mice injected s.c. with a mixture of hPBMCs, tumor cells, and one/tenth of the indicated Ab dose. Subsequently, mice were injected i.v. with the indicated doses twice a week for 3 wk. All mice in Namalwa_CD200, Namalwa_CD200 plus hPBMCs, or 20 mg/kg control Ab groups developed tumors (10 of 10), whereas none of the 10 mice in the 5 mg/kg chB7-G2G4 group and two of the 10 mice in the 5 mg/kg chB7-G1 group developed tumors by day 25, $n = 10$ per group. Error bars represent mean ± SEM; *, $p < 0.00001$.

doses of 5 and 20 mg/kg (for clarity, Fig. 6 shows 5 mg/kg groups only). Both Ab constructs were highly effective in inhibiting tumor growth. Twenty-five days after tumor cell injection and at the end of Ab treatment, at the 5 mg/kg dose none of the mice treated with chB7-G2G4 developed a tumor compared with two of 10 mice treated with chB7-G1. In contrast, at day 25 mice in the negative control Ab-treated group had an average tumor volume of >3500 mm^3. Two weeks after the last Ab treatment, eight of 10 and 10 of 10 mice in the 5 and 20 mg/kg chB7-G1 treated groups, respectively, had developed tumors compared with six of 10 and eight of 10 in the 5 and 20 mg/kg chB7-G2G4 treated groups, respectively. Considering the limited lifespan of hPBMCs in NOD/SCID mice as well as the exhaustion after activation and the lack of renewal of these cells, long-term effects of anti-CD200 treatment cannot be assessed. However, it appears that anti-CD200 treatment for 3 wk was curative in a portion of the mice. In vivo efficacy of the chB7-G2G4 Ab in this study showing 99.5% tumor growth inhibition at a 5 mg/kg dose provides evidence that tumor growth inhibition by anti-CD200 is based on blocking the CD200 receptor-ligand interaction.

Anti-CD200 Ab treatment inhibits tumor growth in the CD200_Namalwa model when Ab treatment is initiated after ligand-receptor interactions have occurred

In all of studies described above, Abs were administered to the mice at the same time that they received tumor cells and hPBMCs. Although such a model is important to demonstrate the biologic effect of CD200 on cancer cells, immune cells will have already

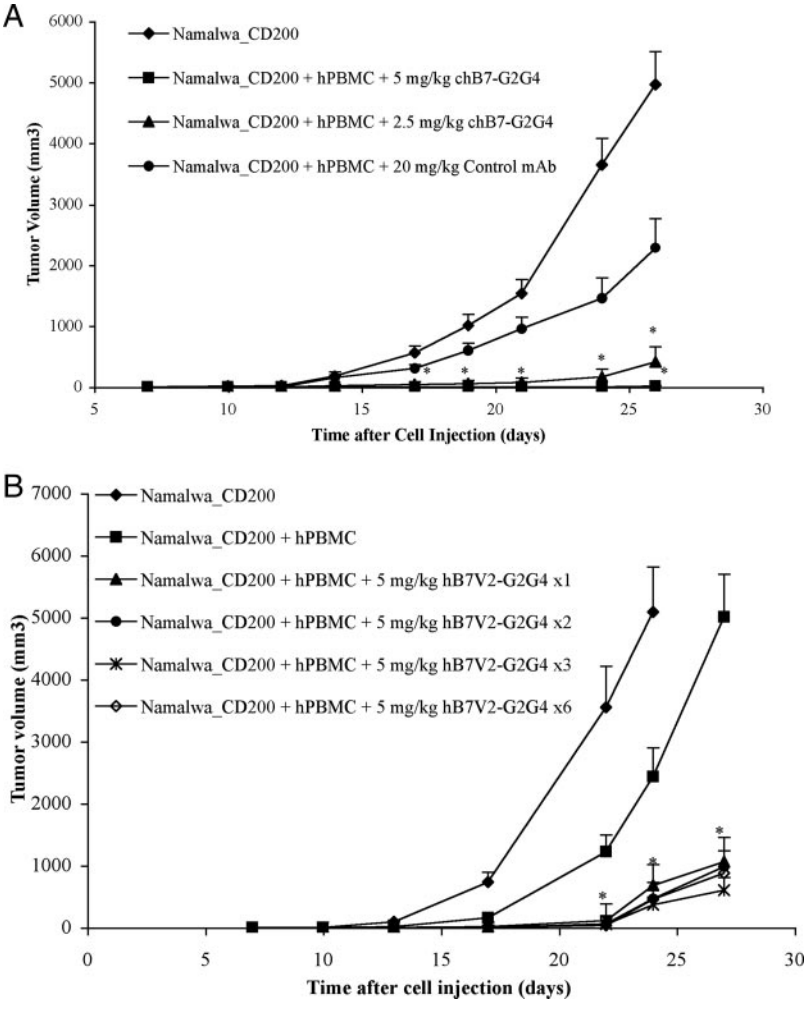

FIGURE 7. Anti-CD200 Ab inhibits tumor growth in the established CD200_Namalwa hPBMC model. NOD/SCID mice were injected with 10×10^6 hPBMCs and 4×10^6 Namalwa_CD200 cells. Ab was first administered i.v. 7 days after tumor cell injection and (*A*) was continued twice a week for 3 wk with tumor incidence of 11 of 11 mice for Namalwa_CD200 (×3), two of 11 mice for 5 mg/kg chB7-G2G4, three of 11 mice for 2.5 mg/kg chB7-G2G4, and 10 of 11 mice for 20 mg/kg control Ab at the end of the study (*B*) or administered only once (×1) with tumor incidence of seven of 10 mice, twice a week for 1 wk (×2) with a tumor incidence of 10 of 10 mice, or once a week over 3 wk (×3) with tumor incidence of 10 of 10 mice or twice a week over 3 wk (×6) with tumor incidence of nine of 10 mice. Error bars represent mean ± SEM; *, $p < 0.00001$.

interacted with CD200 on tumor cells in cancer patients before a therapeutic anti-CD200 Ab can be administered. To investigate whether anti-CD200 treatment is effective after hPBMCs have interacted with CD200 on tumor cells, anti-CD200 treatment was initiated 7 days after NOD/SCID mice were injected with Namalwa_CD200 cells and hPBMCs. Although tumor volumes in mice that received hPBMCs and control Ab were somewhat reduced compared with tumor volumes in mice that received tumor cells only, there was still a large enough window to observe further tumor growth inhibition. Treatment with 5 mg/kg chB7-G2G4 resulted in strong tumor growth inhibition (99.5% at the study's end, day 26, compared with control mAb treated mice), while 2.5 mg/kg had a lesser effect (83% at day 26) (Fig. 7*A*). Only two of 10 or three of 10 mice had a small tumor at day 26 in the 5 mg/kg or 2.5 mg/kg chB7-G2G4 treated groups, respectively. Importantly, these results indicate that anti-CD200 treatment is effective even after hPBMCs have interacted with CD200 on tumor cells.

In a further study, we evaluated whether a single dose of the humanized Ab hB7V2-G2G4 can inhibit tumor growth when treatment is initiated 7 days after tumor cell and hPBMC injection. As shown in Fig. 7*B*, administration of a single dose of 5 mg/kg hB7V2-G2G4 significantly inhibited tumor growth (62%). However, multiple dosing was more effective. Weekly dosing over 3 wk was most effective in inhibiting tumor growth (72%).

Discussion

To evade host immunity, tumors use numerous strategies to hinder the function of critical cells of the immune system. A number of different negative immune regulators expressed on the surface of tumor cells have been identified, such as B7-H1 (23, 24) and B7-H4 (25–27). In this study we provide novel in vivo evidence for another strong inhibitor of an immunological antitumor response. CD200, found on certain tumors such as B-CLL (5), exerts its effects through interaction with its receptor, CD200R. Because CD200R is expressed on macrophages and dendritic cells as well as on certain T cells such as follicular Th cells (17), tumor-expressed CD200 can negatively influence the immune system through multiple pathways.

The best understood function of CD200 based on in vitro data is its effect on macrophages and dendritic cells. Interaction with CD200R on plasmacytoid dendritic cells induces the immunosuppressive pathway of tryptophan catabolism (28). CD200R engagement biases stem cells in the bone marrow toward the development of suppressive APCs, which can induce regulatory T cells (29). Dendritic cells found in cancer patients, including patients with B-CLL, are often defective (30, 31) and detrimental to an effective antitumor response (32). CD200R engagement might be an important factor contributing to their immunosuppressive state. B-CLL cells themselves are weak APCs due to their low levels of costimulatory molecules (33). Enabling immune cells in the tumor cell environment to mount an effective antitumor response by blocking CD200 might be promising because autologous CTLs capable of killing B-CLL cells have been generated in vitro (34–36) and in vivo with autologous tumor cell vaccines (37), indicating that they are present at some level in patients. In the case of B-CLL, tumor cells may have a particularly high impact on the fate of APCs in bone marrow. B-CLL cells home to the marrow via chemo attraction between CXCR-4 on the B-CLL surface and stromal cell-derived factor 1 (SDF-1) in the bone marrow (38). B-CLL cells are also preferentially found in the spleen, another organ where tumor cells can impact a large number of immune cells.

In addition to the effect of CD200 on altering APCs, the observed shift from Th1 to Th2 profiles after CD200R engagement might also play an important role in cancer progression. A shift from Th1 to Th2 cytokine production has been observed during the progression of many cancers and has been associated with a negative prognosis (39–41). Podhorecka et al. (42, 43) showed that a Th1 cytokine response shifts to a Th2 cytokine response during the progression of B-CLL. These cytokine shifts are expected to negatively influence T cell cytotoxicity and the ability of B-CLL cells to undergo apoptosis. Previously, Gorczynki et al. (44) showed in a mouse leukemia model that anti-CD200 treatment of EL4 cells transfected with CD86 can be beneficial. Increased CD200 expression in this model was demonstrated on spleen cells, implying that anti-CD200 in this model affected immune cells. Tumor cells were not evaluated for CD200 expression. However, this effect was not observed with EL4 cells transfected with CD80, indicating that in this model anti-CD200 therapy did not universally increase an antitumor response by blocking CD200 on immune cells. This was also confirmed in our model where tumor growth inhibition was not increased by anti-CD200 treatment of Namalwa or RAJI cells in the absence of CD200 expression on the tumor (data not shown). Our data clearly demonstrate that CD200 expressed on tumor cells can block an antitumor response and that anti-CD200 therapy is effective in our model for tumors expressing CD200, even in the setting where receptor-ligand interactions are already in place at the time of Ab administration. Although an anti-CD200 Ab with an IgG1 constant region could mediate tumor cell killing through the ADCC or CDC activity inherent in the IgG1 constant region, effective tumor cell killing using an anti-CD200 Ab with a hybrid constant region composed of human IgG2 CH1 and hinge region fused to the IgG4 CH2 and CH3 constant regions that cannot mediate ADCC or CDC suggests that the Ab exerts its antitumor activity by blocking the CD200/CD200R interaction. This conclusion was further supported by the lack of a direct effect of the Ab on tumor cells as demonstrated in apoptosis and proliferation assays. Furthermore, microarray experiments did not show the up-regulation of any cellular pathways after incubation of Namalwa_CD200 cells with anti-CD200 Abs (data not shown), indicating that a CD200 receptor-bearing cell is required to see an effect of CD200 modulation. The lack of ADCC and CDC activity and a direct effect on cancer cells distinguishes our anti-CD200 Ab from other clinically used mAbs such as rituximab (anti-CD20) and trastuzumab (anti-HER-2). Both rituximab and trastuzumab have G1 constant regions and have been shown to mediate CDC and ADCC activity in vitro. In the case of anti-CD20, efficient tumor cell killing in patients with non-Hodgkin's lymphoma has more recently been demonstrated to be dependent on FcγRIII alleles (45), further supporting ADCC-mediated killing as one key mechanism. Other mechanisms also play a role (46). CD20 appears to function as a calcium channel, and recent data suggest that Rituxan cross-linking induces the translocation of CD20 to lipid rafts, which is important for increased intracellular calcium levels and downstream apoptotic signaling. Anti-HER-2 Abs target a receptor tyrosine kinase with a signaling domain that is overexpressed and appears to be integrally involved in disease progression (47). Targeting Her2/neu with a bivalent (cross-linking) Ab has an effect on cell proliferation. In contrast, CD200 does not have a signaling domain. All of our studies have demonstrated that the anti-CD200-G2/4 Ab does not block or activate intracellular signaling in the CD200-expressing tumors. Furthermore, the anti-CD200-G2/G4 Ab cannot mediate cell killing through ADCC or CDC due to our engineering of the constant region. Therefore, another cell type (CD200R bearing) is required to see an effect of CD200 modulation. Hence, though immune cell-mediated killing is common among these Abs, their mechanisms are different.

The animal model we describe herein, where mice are reconstituted with human immune cells and human tumor cells, is a broadly applicable useful model for the study of various human targets and new therapeutic agents that play a role in immune modulation. It provides a system for the evaluation of key pathways where differences between the mouse and human immune system are known, as well as for the study of therapeutic Abs and other reagents that do not cross-react with their targets in rodents. Although ideally primary B-CLL cells or a B-CLL cell line would serve as source of tumor cells, such a system has not been consistently established. We previously created a B-CLL cell line (5) that was used to identify CD200 as a cell surface target on B-CLL cells. Interestingly, the B-CLL cell line that we created, which originally expressed CD200, down-regulated it in vitro, and the addition of various cytokines in vitro had no effect on the level of CD200 expression. The cell line showed tumor growth in vivo only when injected together with hPBMCs, suggesting potential effects of a growth factor produced by hPBMCs (data not shown). The few tumors that did grow up-regulated CD200 expression. Although it is difficult to directly relate cause and effect, it seems that pressure by the immune system may have resulted in the up-regulation of CD200. In the absence of such pressure in vitro, CD200 is not playing a critical role and is therefore down-regulated. Because tumor incidence was low (40%), this is not a suitable model for testing Ab efficacy.

Although the hPBMC model is suitable for demonstrating the importance of CD200 in the tumor environment and the potential therapeutic value of blocking Abs, the model has limitations in that human immune cells have a limited lifespan in the mouse. Waiting until tumors are large to test an effect of an anti-CD200 Ab is not an option because effector cells are not renewable in this model and insufficient numbers remain after 4 wk. However, the critical question is whether a blocking Ab can provide a therapeutic benefit after the inhibitory interactions between ligand and receptor have occurred. Indeed, we do see a strong therapeutic benefit of administrating anti-CD200 Abs with abrogated effector function even in the face of the inhibitory interactions between CD200 and its receptor that are already in place, similar to the human cancer setting. CD200 down-regulation was observed after 3 wk of anti-CD200 treatment. In stark contrast to most antitumor Ab therapies, treatment-related down-regulation of the target may be a benefit by improving the capacity of human immune cells to eradicate cancer cells.

Although ideally hPBMCs from patients would be studied in this model, insufficient samples are available to perform a thorough study. As an alternative, an allogeneic tumor xenograft model with normal hPBMCs was chosen to demonstrate that the immunosuppressive effect of CD200 is very robust. CD200R is found on similar cell types in B-CLL patients as in normal donors and is present on an average of 30% of PBMCs in B-CLL patients, suggesting that immunosuppressive interactions of CD200 with CD200R can take place in B-CLL patients. Whether CD200 indeed plays such an immunosuppressive role in B-CLL patients can only be addressed in the clinic. The model does however provide a solid scientific rationale for studying the effectiveness of anti-CD200 therapy in patients with B-CLL or other cancers expressing CD200. Consideration of the normal expression profile of CD200 (7) and the proposed mechanism of action of an anti-CD200 Ab in generating an antitumor response suggest that C region selection may be important. An effectorless C-region like the G2G4 fusion could limit the damage of normal cells expressing CD200, such as endothelial cells and neural cells. In contrast, the additional benefit of ADCC and/or CDC activity may increase the potency of immune-mediated tumor cell killing after Ab binding. As with other cancer therapies, a combination of anti-CD200 therapy with cancer vaccines or chemotherapeutics might ultimately be most effective. Interestingly, fludarabine, the current standard therapy for B-CLL, has been shown to reduce the number of regulatory T cells in B-CLL patients (48). A combination of fludarabine with an agent that prevents the induction of regulatory T cells might be very effective. Finally, in contrast to existing B-CLL therapies, anti-CD200 therapy may stimulate the immune system to provide an antitumor effect, as well as simultaneously reduce the risk of infections in B-CLL patients.

Taken together, our data provide evidence for immune suppression mediated by CD200 expression on tumors. Administration of an antagonistic anti-CD200 Ab enabled the human immune system to eradicate CD200-expressing cancer cells in our model system. Whether anti-CD200 therapy is a safe and viable approach in the setting of human cancer awaits further study.

Acknowledgments

The expert CD200 library construction and panning efforts by Linh Tran and Kenix Vo are greatly appreciated. David Giess and Krista Johnsson are acknowledged for efficient production and purification of all Abs used in the animal studies. The diligent work on formatting of figures by Jeffrey Sun is appreciated.

Disclosures

All of the authors are stockholders of Alexion. A. Kretz-Rommel, K. S. Bowdish, J. McWhirter, and J. Springhorn are listed as inventors on two pending patents filed by Alexion and titled "Polypeptides and antibodies derived from chronic lymphocytic leukemia cells and uses thereof" and "Antibodies to ox-2/cd200 and uses thereof."

References

1. Zou, W. 2005. Immunosuppressive networks in the tumour environment and their therapeutic relevance. *Nat. Rev. Cancer* 5: 263–274.
2. Frey, A. B., and N. Monu. 2006. Effector-phase tolerance: another mechanism of how cancer escapes antitumor immune response. *J. Leukocyte Biol.* 79: 652–662.
3. Phan, G. Q., J. C. Yang, R. M. Sherry, P. Hwu, S. L. Topalian, D. J. Schwartzentruber, N. P. Restifo, L. R. Haworth, C. A. Seipp, L. J. Freezer, et al. 2003. Cancer regression and autoimmunity induced by cytotoxic T lymphocyte-associated antigen 4 blockade in patients with metastatic melanoma. *Proc. Natl. Acad. Sci. USA* 100: 8372–8377.
4. Ribas, A., L. H. Camacho, G. Lopez-Berestein, D. Pavlov, C. A. Bulanhagui, R. Millham, B. Comin-Anduix, J. M. Reuben, E. Seja, C. A. Parker, et al. 2005. Antitumor activity in melanoma and anti-self responses in a phase I trial with the anti-cytotoxic T lymphocyte-associated antigen 4 monoclonal antibody CP-675,206. *J. Clin. Oncol.* 23: 8968–8977.
5. McWhirter, J. R., A. Kretz-Rommel, A. Saven, T. Maruyama, K. N. Potter, C. I. Mockridge, E. P. Ravey, F. Qin, and K. S. Bowdish. 2006. Antibodies selected from combinatorial libraries block a tumor antigen that plays a key role in immunomodulation. *Proc. Natl. Acad. Sci. USA* 103: 1041–1046.
6. Barclay, A. N., M. J. Clark, and G. W. McCaughan. 1986. Neuronal/lymphoid membrane glycoprotein MRC OX-2 is a member of the immunoglobulin superfamily with a light-chain-like structure. *Biochem. Soc. Symp.* 51: 149–157.
7. Wright, G. J., M. Jones, M. J. Puklavec, M. H. Brown, and A. N. Barclay. 2001. The unusual distribution of the neuronal/lymphoid cell surface CD200 (OX2) glycoprotein is conserved in humans. *Immunology* 102: 173–179.
8. Barclay, A. N., G. J. Wright, G. Brooke, and M. H. Brown. 2002. CD200 and membrane protein interactions in the control of myeloid cells. *Trends Immunol.* 23: 285–290.
9. Hoek, R. M., S. R. Ruuls, C. A. Murphy, G. J. Wright, R. Goddard, S. M. Zurawski, B. Blom, M. E. Homola, W. J. Streit, M. H. Brown, et al. 2000. Down-regulation of the macrophage lineage through interaction with OX2 (CD200). *Science* 290: 1768–1771.
10. Jenmalm, M. C., H. Cherwinski, E. P. Bowman, J. H. Phillips, and J. D. Sedgwick. 2006. Regulation of myeloid cell function through the CD200 receptor. *J. Immunol.* 176: 191–199.
11. Gorczynski, L., Z. Chen, J. Hu, Y. Kai, J. Lei, V. Ramakrishna, and R. M. Gorczynski. 1999. Evidence that an OX-2-positive cell can inhibit the stimulation of type 1 cytokine production by bone marrow-derived B7-1 (and B7-2)-positive dendritic cells. *J. Immunol.* 162: 774–781.
12. Gorczynski, R. M., L. Lee, and I. Boudakov. 2005. Augmented induction of $CD4^+CD25^+$ Treg using monoclonal antibodies to CD200R. *Transplantation* 79: 488–491.
13. Curiel, T. J., G. Coukos, L. Zou, X. Alvarez, P. Cheng, P. Mottram, M. Evdemon-Hogan, J. R. Conejo-Garcia, L. Zhang, M. Burow, et al. 2004. Specific recruitment of regulatory T cells in ovarian carcinoma fosters immune privilege and predicts reduced survival. *Nat. Med.* 10: 942–949.

14. Gorczynski, R. M., M. S. Cattral, Z. Chen, J. Hu, J. Lei, W. P. Min, G. Yu, and J. Ni. 1999. An immunoadhesin incorporating the molecule OX-2 is a potent immunosuppressant that prolongs allo- and xenograft survival. *J. Immunol.* 163: 1654–1660.
15. Taylor, N., K. McConachie, C. Calder, R. Dawson, A. Dick, J. D. Sedgwick, and J. Liversidge. 2005. Enhanced tolerance to autoimmune uveitis in CD200-deficient mice correlates with a pronounced Th2 switch in response to antigen challenge. *J. Immunol.* 174: 143–154.
16. Gorczynski, R., Z. Chen, Y. Kai, L. Lee, S. Wong, and P. A. Marsden. 2004. CD200 Is a ligand for all members of the CD200R family of immunoregulatory molecules. *J. Immunol.* 172: 7744–7749.
17. Wright, G. J., H. Cherwinski, M. Foster-Cuevas, G. Brooke, M. J. Puklavec, M. Bigler, Y. Song, M. Jenmalm, D. Gorman, T. McClanahan, et al. 2003. Characterization of the CD200 receptor family in mice and humans and their interactions with CD200. *J. Immunol.* 171: 3034–3046.
18. Wild, M. A., H. Xin, T. Maruyama, M. J. Nolan, P. M. Calveley, J. D. Malone, M. R. Wallace, and K. S. Bowdish. 2003. Human antibodies from immunized donors are protective against anthrax toxin in vivo. *Nat. Biotechnol.* 21: 1305–1306.
19. Mueller, J. P., M. A. Giannoni, S. L. Hartman, E. A. Elliott, S. P. Squinto, L. A. Matis, and M. J. Evans. 1997. Humanized porcine VCAM-specific monoclonal antibodies with chimeric IgG2/G4 constant regions block human leukocyte binding to porcine endothelial cells. *Mol. Immunol.* 34: 441–452.
20. Epstein, M. A., B. G. Achong, Y. M. Barr, B. Zajac, G. Henle, and W. Henle. 1966. Morphological and virological investigations on cultured Burkitt tumor lymphoblasts (strain Raji). *J. Natl. Cancer Inst.* 37: 547–559.
21. Klein, G., L. Dombos, and B. Gothoskar. 1972. Sensitivity of Epstein-Barr virus (EBV) producer and non-producer human lymphoblastoid cell lines to superinfection with EB-virus. *Int. J. Cancer* 10: 44–57.
22. Teeling, J. L., R. R. French, M. S. Cragg, J. van den Brakel, M. Pluyter, H. Huang, C. Chan, P. W. Parren, C. E. Hack, M. Dechant, et al. 2004. Characterization of new human CD20 monoclonal antibodies with potent cytolytic activity against non-Hodgkin lymphomas. *Blood* 104: 1793–1800.
23. Dong, H., S. E. Strome, D. R. Salomao, H. Tamura, F. Hirano, D. B. Flies, P. C. Roche, J. Lu, G. Zhu, K. Tamada, et al. 2002. Tumor-associated B7-H1 promotes T-cell apoptosis: a potential mechanism of immune evasion. *Nat. Med.* 8: 793–800.
24. Curiel, T. J., S. Wei, H. Dong, X. Alvarez, P. Cheng, P. Mottram, R. Krzysiek, K. L. Knutson, B. Daniel, M. C. Zimmermann, et al. 2003. Blockade of B7-H1 improves myeloid dendritic cell-mediated antitumor immunity. *Nat. Med.* 9: 562–567.
25. Sica, G. L., I. H. Choi, G. Zhu, K. Tamada, S. D. Wang, H. Tamura, A. I. Chapoval, D. B. Flies, J. Bajorath, and L. Chen. 2003. B7-H4, a molecule of the B7 family, negatively regulates T cell immunity. *Immunity* 18: 849–861.
26. Prasad, D. V., S. Richards, X. M. Mai, and C. Dong. 2003. B7S1, a novel B7 family member that negatively regulates T cell activation. *Immunity* 18: 863–873.
27. Kryczek, I., L. Zou, P. Rodriguez, G. Zhu, S. Wei, P. Mottram, M. Brumlik, P. Cheng, T. Curiel, L. Myers, et al. 2006. B7-H4 expression identifies a novel suppressive macrophage population in human ovarian carcinoma. *J. Exp. Med.* 203: 871–881.
28. Fallarino, F., C. Asselin-Paturel, C. Vacca, R. Bianchi, S. Gizzi, M. C. Fioretti, G. Trinchieri, U. Grohmann, and P. Puccetti. 2004. Murine plasmacytoid dendritic cells initiate the immunosuppressive pathway of tryptophan catabolism in response to CD200 receptor engagement. *J. Immunol.* 173: 3748–3754.
29. Gorczynski, R. M., Z. Chen, Y. Kai, S. Wong, and L. Lee. 2004. Induction of tolerance-inducing antigen-presenting cells in bone marrow cultures in vitro using monoclonal antibodies to CD200R. *Transplantation* 77: 1138–1144.
30. Takahashi, S., H. Mok, M. B. Parrott, F. C. Marini III, M. Andreeff, M. K. Brenner, and M. A. Barry. 2003. Selection of chronic lymphocytic leukemia binding peptides. *Cancer Res.* 63: 5213–5217.
31. Orsini, E., A. Guarini, S. Chiaretti, F. R. Mauro, and R. Foa. 2003. The circulating dendritic cell compartment in patients with chronic lymphocytic leukemia is severely defective and unable to stimulate an effective T-cell response. *Cancer Res.* 63: 4497–4506.
32. Mohty, M., D. Olive, and B. Gaugler. 2002. Leukemic dendritic cells: potential for therapy and insights towards immune escape by leukemic blasts. *Leukemia* 16: 2197–2204.
33. Buhmann, R., C. Kurzeder, J. Rehklau, D. Westhaus, S. Bursch, W. Hiddemann, T. Haferlach, M. Hallek, and C. Schoch. 2002. CD40L stimulation enhances the ability of conventional metaphase cytogenetics to detect chromosome aberrations in B-cell chronic lymphocytic leukaemia cells. *Br. J. Haematol.* 118: 968–975.
34. Hami, L. S., C. Green, N. Leshinsky, E. Markham, K. Miller, and S. Craig. 2004. GMP production and testing of Xcellerated T cells for the treatment of patients with B-CLL. *Cytotherapy* 6: 554–562.
35. Trojan, A., J. L. Schultze, M. Witzens, R. H. Vonderheide, M. Ladetto, J. W. Donovan, and J. G. Gribben. 2000. Immunoglobulin framework-derived peptides function as cytotoxic T-cell epitopes commonly expressed in B-cell malignancies. *Nat. Med.* 6: 667–672.
36. Goddard, R. V., A. G. Prentice, J. A. Copplestone, and E. R. Kaminski. 2001. Generation in vitro of B-cell chronic lymphocytic leukaemia-proliferative and specific HLA class-II-restricted cytotoxic T-cell responses using autologous dendritic cells pulsed with tumour cell lysate. *Clin. Exp. Immunol.* 126: 16–28.
37. Gitelson, E., C. Hammond, J. Mena, M. Lorenzo, R. Buckstein, N. L. Berinstein, K. Imrie, and D. E. Spaner. 2003. Chronic lymphocytic leukemia-reactive T cells during disease progression and after autologous tumor cell vaccines. *Clin. Cancer Res.* 9: 1656–1665.
38. Burger, J. A., M. Burger, and T. J. Kipps. 1999. Chronic lymphocytic leukemia B cells express functional CXCR4 chemokine receptors that mediate spontaneous migration beneath bone marrow stromal cells. *Blood* 94: 3658–3667.
39. Tendler, C. L., J. D. Burton, J. Jaffe, D. Danielpour, M. Charley, J. P. McCoy, M. R. Pittelkow, and T. A. Waldmann. 1994. Abnormal cytokine expression in Sezary and adult T-cell leukemia cells correlates with the functional diversity between these T-cell malignancies. *Cancer Res.* 54: 4430–4435.
40. Takeuchi, T., T. Ueki, Y. Sasaki, T. Kajiwara, B. Li, N. Moriyama, and K. Kawabe. 1997. Th2-like response and antitumor effect of anti-interleukin-4 mAb in mice bearing renal cell carcinoma. *Cancer Immunol. Immunother.* 43: 375–381.
41. Lauerova, L., L. Dusek, M. Simickova, I. Kocak, M. Vagundova, J. Zaloudik, and J. Kovarik. 2002. Malignant melanoma associates with Th1/Th2 imbalance that coincides with disease progression and immunotherapy response. *Neoplasma* 49: 159–166.
42. Podhorecka, M., A. Dmoszynska, J. Rolinski, and E. Wasik-Szczepanek. 2001. Intracellular interleukin-2 expression by T-cell subsets in B-cell chronic lymphocytic leukemia. *Haematologica* 86: 549–550.
43. Podhorecka, M., A. Dmoszynska, J. Rolinski, and E. Wasik. 2002. T type 1/type 2 subsets balance in B-cell chronic lymphocytic leukemia—the three-color flow cytometry analysis. *Leuk. Res.* 26: 657–660.
44. Gorczynski, R. M., Z. Chen, J. Hu, Y. Kai, and J. Lei. 2001. Evidence of a role for CD200 in regulation of immune rejection of leukaemic tumour cells in C57BL/6 mice. *Clin. Exp. Immunol.* 126: 220–229.
45. Cartron, G., L. Dacheux, G. Salles, P. Solal-Celigny, P. Bardos, P. Colombat, and H. Watier. 2002. Therapeutic activity of humanized anti-CD20 monoclonal antibody and polymorphism in IgG Fc receptor FcγRIIIa gene. *Blood* 99: 754–758.
46. Cartron, G., H. Watier, J. Golay, and P. Solal-Celigny. 2004. From the bench to the bedside: ways to improve rituximab efficacy. *Blood* 104: 2635–2642.
47. Albanell, J., J. Codony, A. Rovira, B. Mellado, and P. Gascon. 2003. Mechanism of action of anti-HER2 monoclonal antibodies: scientific update on trastuzumab and 2C4. *Adv. Exp. Med. Biol.* 532: 253–268.
48. Beyer, M., M. Kochanek, K. Darabi, A. Popov, M. Jensen, E. Endl, P. A. Knolle, R. K. Thomas, M. von Bergwelt-Baildon, S. Debey, et al. 2005. Reduced frequencies and suppressive function of $CD4^+$ $CD25^{high}$ regulatory T cells in patients with chronic lymphocytic leukemia after therapy with fludarabine. *Blood* 106: 2018–2025.